

Goal-Driven Autonomous Mapping Through Deep Reinforcement Learning and Planning-Based Navigation

Reinis Cimurs¹, Il Hong Suh², and Jin Han Lee²

Abstract—In this paper, we present a goal-driven autonomous mapping and exploration system that combines reactive and planned robot navigation. First, a navigation policy is learned through a deep reinforcement learning (DRL) framework in a simulated environment. This policy guides an autonomous agent towards a goal while avoiding obstacles. We develop a navigation system where this learned policy is integrated into a motion planning stack as the local navigation layer to move the robot towards the intermediate goals. A global path planner is used to mitigate the local optimum problem and guide the robot towards the global goal. Possible intermediate goal locations are extracted from the environment and used as local goals according to the navigation system heuristics. The fully autonomous navigation is performed without any prior knowledge while mapping is performed as the robot moves through the environment. Experiments show the capability of the system navigating in previously unknown surroundings and arriving at the designated goal.

I. INTRODUCTION

Over the last couple of decades, the field of simultaneous localization and mapping (SLAM) has been extensively studied. Typically, in SLAM systems a measuring device is driven by a human operator and a map is generated based on the location and the environmental features or landmarks [1]. However, it is not always possible to manually operate the device due to various reasons - physical constraints, limited resources, environmental dangers, poor connectivity, and so on. Subsequently, autonomous exploration and mapping is an area that is garnering a lot of attention with ongoing research in the ability to delegate the navigation and mapping tasks to an autonomous device such as a robot. Planning-based navigation approaches require initial information about the environment to calculate motion strategies [2]. But for exploration and mapping tasks in unknown or uncertain environments, alternative ways to obtain motion strategies are necessary.

With the recent advances in deep reinforcement learning (DRL) for autonomous robot navigation high-precision decision-making has become feasible to be carried out by autonomous agents. Using DRL, a policy can be learned to control an agent so that the target task is achieved in an unknown environment [3]. By applying learned policy to an

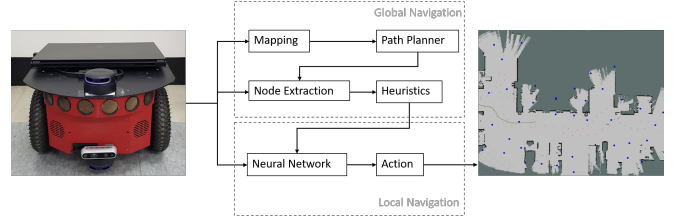


Fig. 1. Navigation system implementation. Robot setup is depicted on the left. Global and local navigation with their respective parts and data flow is visualized in the middle. The mapped environment is presented on the right.

input it is possible to navigate a robot in the environment, without creating a prior plan. However, due to its reactive nature and lack of global information, it easily encounters the local optimum problem, especially for large scale navigation tasks [4]. Therefore, in order to achieve a fully autonomous mapping and exploration, one needs not only agents that can learn to navigate in its vicinity but also a way to guide their motion towards a global goal.

In this paper, we present an autonomous navigation system for mapping towards a specified goal which combines path planning with learned reactive navigation. An initial plan is calculated for navigation towards the selected intermediate goal. Then, local reactive navigation is performed based on the policy, learned through DRL. The main contributions of this work can be itemized as follows:

- Designed and implemented a fully autonomous robot navigation system for exploration and mapping.
- Integrated a DRL-based local navigation into a navigation stack.
- Combined reactive and planned robot navigation and performed extensive experiments to validate its viability.

The remainder of this paper is organized as follows. In Section II related works are reviewed. The proposed navigation and mapping system is described in Section III. Experimental results are given in Section IV. Finally, this paper concludes in Section V.

II. RELATED WORKS

Environmental exploration and mapping has been a popular study in the field of robotics for decades [5], [6], [7]. With the availability of various low-cost sensors and computational devices, it has become increasingly possible to perform SLAM on the robotic agent in real-time with a number of different approaches. Sensor devices such as cameras [8], [9], [10], two dimensional [11], [12], [13] and three dimensional LiDARs [14], [15], [16], and their combinations [17], [18], [19] are used not only to detect

*This work was supported by the Technology Innovation Program (Industrial Strategic Technology Development, 10080638) funded by the Ministry of Trade, Industry & Energy (MOTIE), Republic of Korea.

¹R. Cimurs is with Department of Intelligent Robot Engineering, Hanyang University, Republic of Korea; reinis@incorl.hanyang.ac.kr

²J.H. Lee, I.H. Suh are with the Department of Electronics and Computer Engineering, Hanyang University, Republic of Korea {jinhanlee, ihsuh}@hanyang.ac.kr

and record the environment but also to autonomously locate the agents' position within it. However, to obtain reliable map information of the surroundings through navigation, a large portion of developed SLAM systems rely on human operators or a pre-described plan [20], [21], [22]. Also, many autonomous exploration approaches are developed based on previously available map [23], [24], [25]. Exploration directions are extracted from the map edges that show free space in the environment. Subsequently, a navigation plan is created towards the selected goal, and navigation performed according to it [26], [27], [28].

Due to the rise in popularity and the capabilities of deep learning methods, highly reliable robot navigation through neural networks has been developed. Robots are able to perform deliberate motions obtained directly from neural-network outputs. In [29] the work maps the environment by using learned predictions of the frontier areas that guide the exploration of the robot. But the navigation is still carried out based on a planner. Exploratory navigation through deep Q-learning is presented in [30], where a robot learns to avoid obstacles while navigating straight in unknown environments. This is further extended in [31], where a robot learns an obstacle-avoiding policy in a simulation and the network is applied to real-world environments. Here, navigation actions are defined only in discrete space without a specific goal. Robot actions in continuous action space are obtained by performing learning in deep deterministic policy gradient-based (DDPG) networks. Here, the environmental state information is combined with the goal position to form the input for the network [32], [33]. However, since the information about the environment is given locally in time and space, they may encounter a local optimum problem when trying to maximize the reward. Even though these methods provide high accuracy and reliability in their respective domains, it is difficult to deploy them in practice due to concerns relating to safety, generalization ability, local optimum problem, and others. As such, these neural network-based methods can tackle modular tasks, but might not be suitable for implementation in global end-to-end solutions. In [34], the behavior-based learned navigation is successfully integrated with planned navigation. However, local planners are still used for motion planning and the neural network is used only to avoid dynamic obstacles, detected from camera images within a previously mapped environment. Similarly, in [35], [36] creation of a local plan is learned and combined with a global path to arrive at a goal and avoid obstacles along the way. Here, a local path is calculated through a neural network in an already mapped environment and exploration is not considered.

Therefore, we propose including the learned navigation as a light-weight module in a broader navigation system and extend it to solve a goal-driven exploration problem. Our aim is not only to navigate around obstacles but also to map and explore an unknown environment towards a specified goal. The proposed fully autonomous system is presented in Fig. 1.

III. GOAL DRIVEN AUTONOMOUS MAPPING

To achieve autonomous navigation and mapping in an unknown environment we propose an autonomous navigation structure that consists of three parts: a deep reinforcement learning-based local navigation, planning-based global navigation, and mapping. At every step, the destination goal point is given to the robot in the form of the x and y coordinates relative to its current location. Mapping is performed while moving between intermediate points towards the global goal, where these points are obtained and selected following the global navigation strategy.

A. Local Navigation

In a planning-based navigation stack, local motion is performed following the local planner. In our approach, we replace this layer of navigation stack with learned policy. We employ DRL to train the local navigation policy separately in a simulated environment.

A DDPG-based neural network architecture is used to train the navigation policy [37]. DDPG is an actor-critic network that allows performing actions in continuous action space. Similarly to [38], the local environment is described by bagged laser readings in 180° range in front of the robot. This information is combined with polar coordinates of the goal with respect to the robot's position. The combined data is used as an input state s in the actor-network of the DDPG. The actor-network consists of two fully connected (FC) layers. Rectified linear unit (ReLU) activation follows after each of these layers. The last layer is then connected to the output layer with two action parameters a that represent the linear velocity a_1 and angular velocity a_2 of the robot. A hyperbolic tangent activation function is applied to the output layer to limit it in the range $(-1, 1)$. Before applying the action in the environment, it is scaled by the maximum linear velocity v_{max} and the maximum angular velocity ω_{max} as follows:

$$a = \left[v_{max} \left(\frac{a_1 + 1}{2} \right), \omega_{max} a_2 \right]. \quad (1)$$

Since the laser readings only record data in front of the robot, motion backwards is not considered and the linear velocity is adjusted to only be positive.

The Q value of the state-action pair $Q(s, a)$ is evaluated in the critic-network. The critic-network uses a pair of the state s and action a as an input. The state s is fed into a fully connected layer followed by ReLU activation with output l_s . The output of this layer, as well as the action, are fed into two separate transformation fully connected layers (TFC) of the same size τ_1 and τ_2 , respectively. These layers are then combined as follows:

$$l_c = l_s W_{\tau_1} + a W_{\tau_2} + b_{\tau_2}, \quad (2)$$

where l_c is the combined fully connected layer (CFC), W_{τ_1} and W_{τ_2} are the weights of the τ_1 and τ_2 , respectively. b_{τ_2} is bias of layer τ_2 . Then ReLU activation is applied on the combined layer. Afterward, it is connected to the output with 1 parameter representing the Q value. The full network architecture is visualized in Fig. 2.

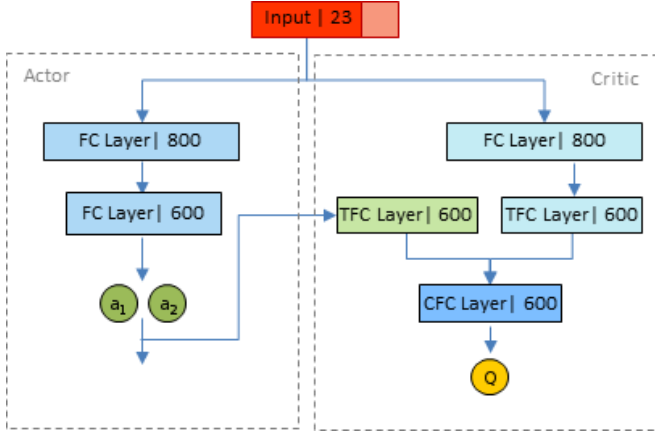


Fig. 2. DDPG network structure including the actor and critic parts. Layer type and the number of their respective parameters are described within the layers. Actor output is represented by the green circles, critics Q-value output by the yellow circle. TFC layers refer to transformation fully connected layers τ and CFC layer to combined fully connected layer l_c .

The policy is rewarded based on the following reward function:

$$r(s_t, a_t) = \begin{cases} r_g & \text{if } D_t < \eta_D \\ r_c & \text{if collision} \\ v - |\omega| & \text{otherwise,} \end{cases} \quad (3)$$

where the reward r of the state-action pair (s_t, a_t) at timestep t is dependant on three conditions. If the distance to the goal at the current timestep D_t is less than the threshold η_D , a positive goal reward r_g is applied. If a collision is detected, a negative collision reward r_c is applied. If both of these conditions are not present, an immediate reward based on the current linear and angular velocities is applied. In order to guide the navigation policy towards the given goal, a delayed attributed reward method is employed based on the following calculation:

$$r_{t-i} = r(s_{t-i}, a_{t-i}) + \frac{r_g}{i}, \quad \forall i = \{1, 2, 3, \dots, n\}, \quad (4)$$

where n is the number of previous steps where rewards would be updated. This means that the positive goal reward will be attributed not only to the state-action pair at which the goal was reached, but also decreasingly over the last n steps before it. The network learned a local navigation policy that is capable of arriving at a local goal, while simultaneously avoiding obstacles directly from the laser inputs.

B. Global Navigation

For a robot to be able to navigate towards a goal at a large distance, intermediate points need to be found as local waypoints for the local navigation. As there is no initial information about the environment, it is not possible to calculate an optimal path or even ensure that the goal is reachable following it. Therefore, the robot needs not only to be guided towards the destination but also to explore the environment along the way to recognize possible alternative routes if it were to encounter a dead-end. Since no prior information is given, the possible navigation points need to be extracted from the immediate surroundings of the robot

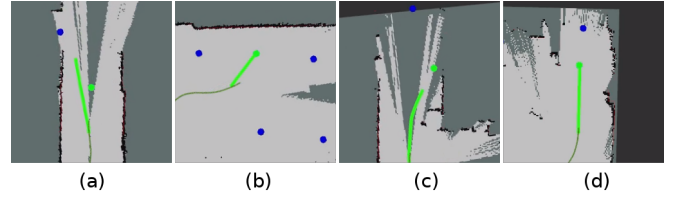


Fig. 3. Node extraction from the environment. Blue circles represent a node, green circles represent the current intermediate goal, the bright green path is the path planner output, dark green path is the odometry of the robot. (a) Blue node is extracted from a gap between laser readings. (b) Blue nodes are extracted from the free space of the environment. (c) Blue node extracted from non-numerical laser readings. (d) Green node extracted from a path planner, that planned a path to the blue node.

and stored in the memory. We will refer to these points as nodes. We implement four methods of obtaining new nodes:

- A node is added if a value difference between two sequential laser readings is larger than a threshold, allowing the robot to navigate through the presumed gap.
- A node is added in the free space of the environment if multiple sequential laser readings values are larger than a threshold.
- Due to laser sensors having maximum range, the readings outside of this range are returned as a non-numerical type and represent free space in the environment. A node is placed in the environment if sequential laser readings return a non-numerical value.
- If a currently selected intermediate goal is too far from the robot's position, a path planner is employed to find a path towards it, and a new node is placed along it.

Examples of node extraction from the environment are depicted in Fig. 3. If in subsequent steps the node is found to be located near an obstacle it is deleted from the memory. Additionally, if a node is selected as an intermediate goal but cannot be reached over a number of steps, this node will be deleted and a new goal node selected. The new nodes obtained from the laser readings are not added to the memory if they are located at a place that the robot has already visited. However, the node obtained from the path planner will be added in such a case to enable back-tracking. All the node coordinates are obtained relative to the robot's position at the current timestep in the map frame.

After obtaining the nodes in the environment, the intermediate goal for local navigation is selected by the following three-level heuristic:

$$h_i = D_{1,i} + D_{2,i}, \quad (5)$$

where value D_2 for the node i is expressed as the Euclidean distance from the node to the global goal. The value of D_1 is calculated as:

$$D_1 = \begin{cases} 0 & \text{if } d(p_r, p_n) < \eta' \\ \eta' & \text{if } \eta' \leq d(p_r, p_n) < \eta'' \\ d(p_r, p_n) & \text{otherwise,} \end{cases} \quad (6)$$

where η' and η'' are the first and second level thresholds, respectively. $d(p_r, p_n)$ is the Euclidean distance between position of the robot p_r and the position of the node p_n .

This heuristic allows selecting a locally reachable node with the smallest distance to the global goal while prioritizing the nodes close to the robot.

C. Mapping and Planning

Following the nodes, the environment is explored and mapped and the robot is guided towards the global goal. Mapping uses laser and robot odometry sensors as sources. However, over time the difference between the internal odometry and map frames begins to drift. To update the node positions in the current map frame, this drift needs to be accounted for. The discrepancy of the frames is different at every timestep. Therefore, when saving the nodes in the memory, they are first transformed with respect to odometry frame at the respective timestep as follows:

$$p'_n = (p_n - T_t)R_t. \quad (7)$$

Here, p'_n represents the updated position. T_t and R_t are translation and rotation matrices from the map to odometry frame at timestep t . While evaluating the heuristic of the node, it is again transformed with respect to the map frame at the current time step as follows:

$$p''_n = -R_t p'_n + T_t. \quad (8)$$

This assures that the nodes as well as the global goal are consistent with the current map.

When a node is selected as the current intermediate goal, a path to it is requested from a global path planner. The Dijkstra algorithm path planner ensures the globally optimal solution towards the goal, based on the current information [39]. If the selected node is located outside of the local navigation range, a new node will be added to the memory at a reachable distance along the global path. Using a path planner allows the robot to backtrack over a previously mapped environment. Additionally, if the selected node is located in an unknown part of the partially mapped environment, the robot can be guided away from the local optimum by following the path.

IV. EXPERIMENTS

To validate the proposed navigation system, experiments in real-life settings of varying complexity were executed.

A. System Setup

The learning of local navigation through DRL was performed on a computer equipped with NVIDIA GTX 1080 graphics card, 32 GB of RAM, and Intel Core i7-6800K CPU. The training of the network was carried out in the Gazebo simulator and controlled by the Robot Operating System (ROS) commands. We trained the network for 800 episodes which took approximately 8 hours. Each training episode consists of 500 steps or until a collision. v_{max} and ω_{max} were set as 0.5 meters per second and 1 radian per second, respectively. The delayed rewards were updated over the last $n = 10$ steps. The training was carried out in a simulated 10x10 meter-sized environment similarly to [33] and depicted in Fig 4. Random noise is added to the sensor

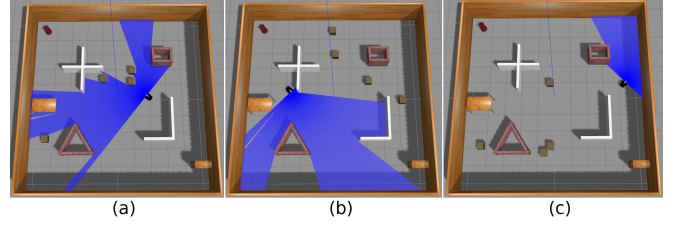


Fig. 4. Examples of training environments. Blue field represents the input laser readings and range. The four box obstacles change their location on every episode as presented in (a), (b), and (c) in order to randomize the training data.

and action values to facilitate generalization and exploration. To further improve the variety of the environment, the location of the box-shaped obstacles were randomized at the start of each episode. Their changing locations are depicted in Fig. 4(a),(b) and (c). The robots starting position as well as the goal locations are randomized on every episode. For quantitative experiments and comparison with similar methods with constrained resources, the network was transferred to an Intel NUC mini-PC (2.70 GHz i7-8559U CPU, 16GB of RAM) that facilitated the full navigation system. For qualitative experiments, the system was embedded on a laptop with NVIDIA RTX 2070M graphics card, 16 GB of RAM, and Intel Core i9-10980HK CPU running Ubuntu 18.04 operating system. ROS Melodic version managed the packages and control commands. Pioneer 3-DX mobile platform was used as the base to carry out the navigation. A two-dimensional laser sensor is capable of only registering data on a single plane at its height. Therefore, to ensure safe navigation we equipped the robot with two RPLidar laser sensors at different heights with a maximal measuring distance of 10 meters. The location and angle of both lasers were calibrated and laser readings recorded in 180° in front of the robot. The data from each device was bagged in 21 groups, where the minimum value of each group was selected as the representative sensor value. Then, the minimal value of each respective bag from both devices was selected to create the final laser input state of 21 values. This allows for the local navigation system to react to obstacles on two planes simultaneously. The final laser data is then combined with the polar coordinates of the intermediate goal. The mapping of the environment was performed based on the full laser readings of only the upper RPLidar sensor in combination with the internal mobile robot odometry. ROS package SLAM Toolbox [40] is used to obtain and update the global map of the environment as well as localize the robot within it. SLAM Toolbox is capable of mapping large-scale environments without sudden jumps in the robot's estimated position. This allows for tracking the robot towards the initial global goal. The scale of the frame drift is obtained by the ROS TF package. The global path is obtained from the ROS package NavFn. An additional Realsense D435 camera was installed on the front of the robot to record the robot's motions. Robot setup is displayed in Fig. 1. Maximal linear and angular velocities were set to the same values as in the simulation. Robot's local navigation range was selected as 5 meters. η' and η'' values were selected as 5

TABLE I
RESULTS OF THE FIRST QUANTITATIVE EXPERIMENT

	Av. Dist.(m)	Av. T.(s)	Min. Dist.(m)	Min. T.(s)	Max. Dist.(m)	Max. T.(s)	σ (Dist.)	σ (T)	Av. Map(m ²)	Goals
GD-RL	77.02	171.82	70.17	147.07	79.49	184.98	3.86	14.96	580.63	5/5
NF	40.74	109.11	34.67	74.6	50.5	150.25	6.73	29.31	475.75	5/5
LP-AM	40.02	123.56	35.43	96.48	46.02	155.4	4.95	25.49	491.57	5/5
GDAM	41.42	88.03	34.77	68.24	54.06	118.05	8.33	20.42	492.01	5/5
PP	32.26	61.53	32.03	59.52	32.32	63.88	0.22	1.89	-	5/5

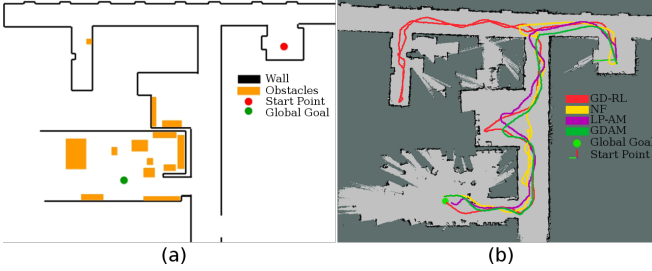


Fig. 5. Environment and resulting navigation examples of the respective methods in the first quantitative experiment. (a) Depiction of the experiment environment. (b) Example of a resulting map of the environment with overlaid path of each method.

and 10 meters, respectively. To ensure smooth navigation, acceleration was constrained for linear and angular velocities. The intermediate goals are considered reached at a 1-meter distance and the global goal at 1.5 meters.

B. Quantitative Experiments

In order to quantify-ably evaluate the proposed method we compare it to different methods of exploring an environment towards a specified goal in indoor settings. We refer to the proposed method as Goal-Driven Autonomous Exploration (GDAM) which combines reinforcement learning with planning to achieve its goal. We compare this with a reinforcement learning-based method without the planning module referred to as Goal Driven Reinforcement Learning (GD-RL). To compare an only planning-based method, we employ Nearest Frontier (NF) exploration strategy from [41]. Here, the distance factor for the nearest frontier also includes the distance to the goal. The planning is performed by the NavFn package. Additionally, we perform experiments with the proposed navigation system where the DDPG network is substituted with a local planner from TrajectoryPlanner ROS package. We refer to this system as Local Planner Autonomous Exploration (LP-AM). Finally, as a baseline comparison we obtain and execute a path obtained from NavFn planner in an already known map. We refer to this method as Path Planner (PP). Experiments are performed in two environments five times with each method. The recorded data includes travel distance (Dist.) in meters, travel time (T) in seconds, recorded map size in square meters and how many times has the method successfully reached the goal. We calculate the average (Av.), maximal (max.), minimal (min.), and standard deviation (σ) of the results. The recorded map size is calculated only from known pixels. In the experiments, the robots starting pose is visualized by the coordinate axis, where the red axis represents the positive x-axis, and green - the positive y-axis.

The first environment is depicted in Fig. 5 and consists

mostly of smooth walls with multiple local optima. The goal is located at coordinate (-12,15). While all the methods were able to arrive at the global goal, they do so with differing travel distance and time. GDAM was capable of arriving at the global goal at comparable travel distance with similar methods but did so in less time. The reasoning for this is that when planning based methods (NF and LP-AM) obtain a new goal, the current path needs to be recalculated before the robot can start moving again which is not the case for the proposed method. This is more evident for LP-AM where the current node selection forces the method to constantly recalculate the local trajectory. However, the GD-RL method falls in the local optima trap, from which it escapes by following a wall. This significantly increases the distance and time to the global goal. The results of the experiment are described in Table I.

The second experiment is depicted in Fig. 6 and introduces obstacles of various complexity into the environment, such as - furniture, chairs, tables, glass walls, and others. Start point is located in a local optimum area with a see-through glass wall at height of the top laser. The proposed method successfully and reliably navigates to the global goal in the shortest time and comparable distance. However, the NF method recognized the path through the glass wall and continuously tried to navigate through it on two out of the five runs eventually failing to reach its goal. Even though the lower laser sensor was able to recognize the obstacle, it was not recorded in the map thus creating a loop of the robot constantly trying to navigate through it. Similarly, the LP-AM collided with an obstacle by creating a path through the legs of of a chair. Since chair legs are narrow, they are occasionally detected as sensor noise, thus require multiple readings to be confirmed and recorded as an obstacle. During the first two runs the GD-RL method was unable to escape the local optimum and failed to reach the global goal. In subsequent runs, a human operator intervened as the robot approached the escape from the starting area and guided the robot towards the free space. The obtained results were calculated over the successful runs and are described in Table II.

C. Qualitative Experiments

Additional experiments with GDAM method were performed in various indoor settings. In Fig. 7 three different environments are depicted, where a local optimum needs to be avoided or navigated out of to arrive at the global goal. The drift between the frames can be noticed as the larger axis is visualized in the map frame and the smaller axis in the odometry frame. The blue dots represent the extracted

TABLE II
RESULTS OF THE SECOND QUANTITATIVE EXPERIMENT

	Av. Dist.(m)	Av. T.(s)	Min. Dist.(m)	Min. T.(s)	Max. Dist.(m)	Max. T.(s)	$\sigma(\text{Dist.})$	$\sigma(T)$	Av. Map(m ²)	Goals
GD-RL	73.12	206.02	68.97	172.95	77.37	234.12	4.2	30.88	986.92	3*/5
NF	56.44	188.02	52.81	178.9	63.13	205.78	5.79	15.37	1014.87	3/5
LP-AM	82.59	296.68	56.13	187.16	103.89	431.27	19.73	100.76	1031.25	4/5
GDAM	67.79	156.54	54.31	124.3	79.69	197.0	9.66	27.64	791.6	5/5
PP	50.53	81.16	48.7	79.34	53.32	83.15	2.04	1.6	-	5/5

* Successful only after human interference.

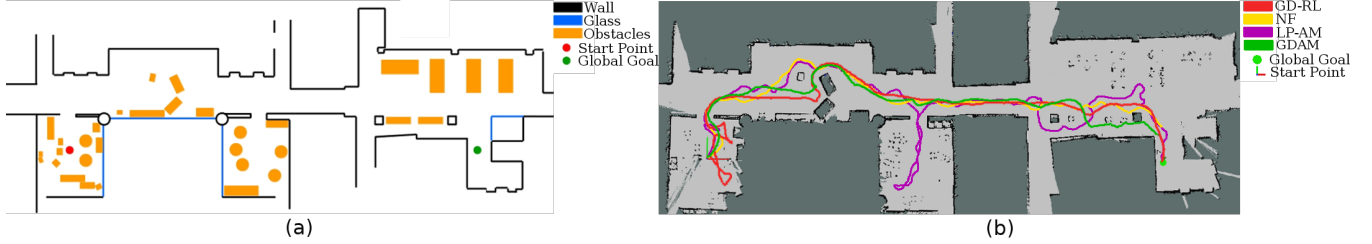


Fig. 6. Environment with more complex obstacles and resulting navigation examples of the respective methods in the second quantitative experiment. (a) Depiction of the experiment environment. (b) Example of a resulting map of the environment with overlaid path of each method.

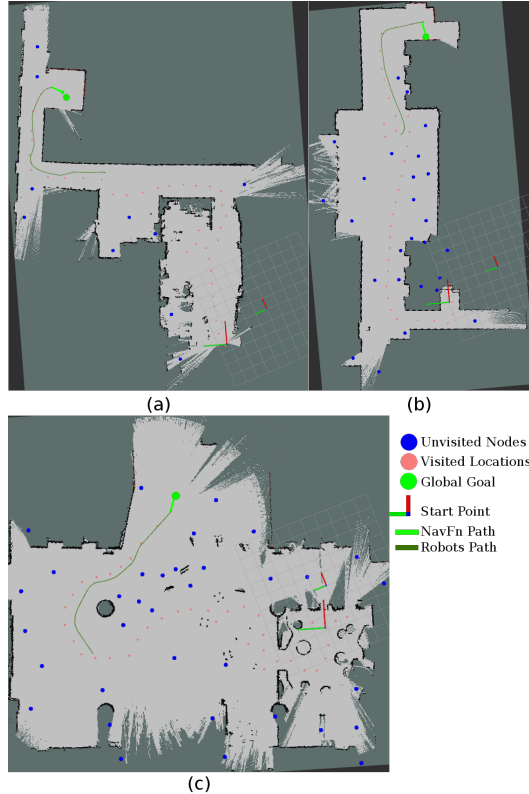


Fig. 7. Experimental results of goal driven exploration and mapping. (a) Navigation towards a goal in hallway. (b) Navigation towards a goal in a hallway, when starting position is in a local optimum. (c) Navigation towards a goal in a hall through a cluttered environment when starting position is in a local optimum.

navigation nodes, orange dots represent the locations the robot has visited. Robot's last 100 steps in the odometry frame are visualized by the dark green path, path planner output is visualized by the bright green path. The global goal is described by a large bright green point. In Fig. 7(a) the goal position is located at coordinate (22, 12) with respect to the robot expressed in meters. A straight path towards the goal leads towards a room corner and a local

optimum. Once the robot has explored the corner, it is able to backtrack, find the exit from the room, and navigate towards the global goal through the hallways. In Fig. 7(b) the goal position is located at coordinate (23, 2) and the robot starting location is placed in the local optimum. Without prior map information and previously extracted nodes, the robot does not have sufficient information for backtracking. By using path planning, a new node is added in the environment, which allows the robot to navigate out of the confined hallway and towards the goal. In Fig. 7(c) the goal coordinates are (10, 10) and the robot starting location is the local optimum. The environment is littered with obstacles of various shapes and sizes, such as chairs, signs, potted plants, and others. The robot successfully explores its surroundings, navigates through the clutter using the local navigation, and arrives at the goal.

Afterwards, navigation and mapping experiments were performed on a larger scale. In Fig. 8 three scenarios are introduced, where a robot navigates towards a goal in hallways and an underground parking lot. In Fig. 8(a) goal is located at coordinate (12, -90). The robot follows the extracted nodes out of the room and navigates towards the goal. Here, the selected intermediate goals are mainly selected from nodes extracted from the free space and the path planner without the need to backtrack to previously seen locations. In Fig. 8(b) goal coordinate is (60, -7). The robot's starting position is located in a cluttered environment and its starting pose is compromised by facing an obstacle. The robot is capable of navigating out of the clutter and moving towards the global goal based on the local information. Once it approaches the wall that blocks direct movement towards the global goal, it explores the local surroundings to find a path. In Fig. 8 the goal is located 100 meters diagonally across an underground parking lot at coordinate (100, 0). The environment is generally free of major obstacles and walls that would appear on a map. However, there is a multitude of parking bumpers at a maximum height of approximately 0.2

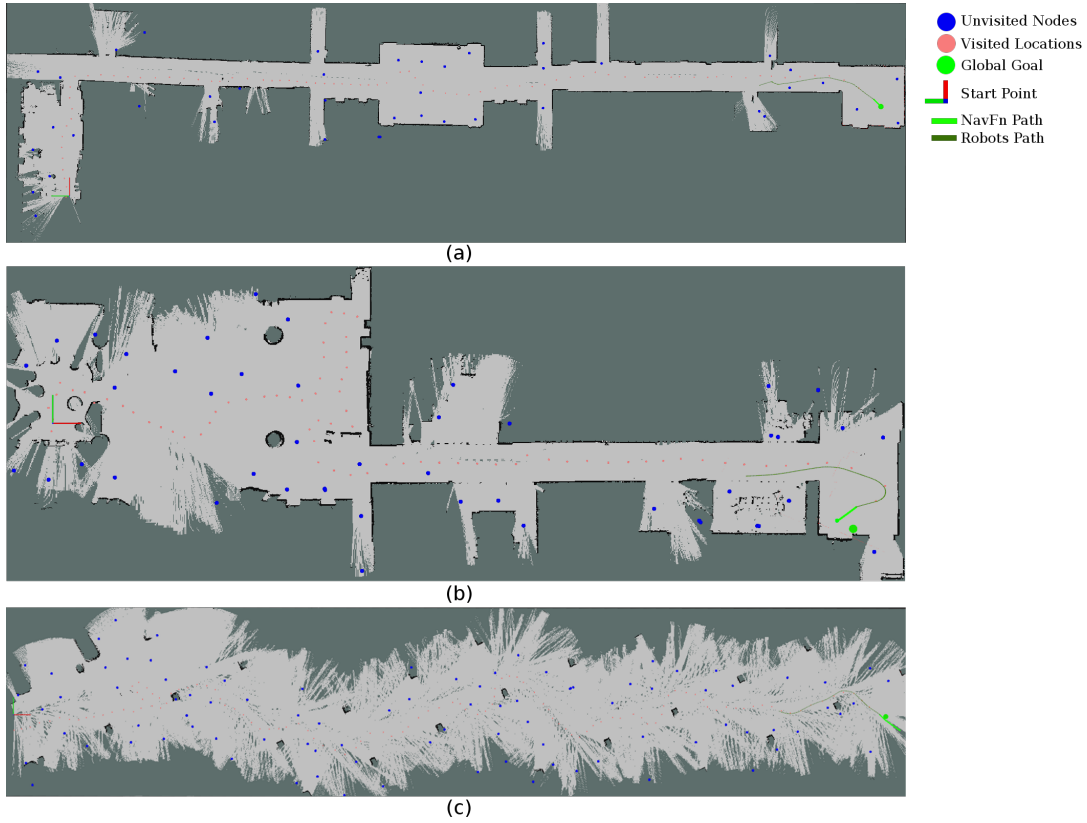


Fig. 8. Experimental results of goal driven exploration and mapping with goal located at a significant distance from the robot. (a) Navigation towards a goal in hallway. (b) Navigation towards a goal in a hall and hallway with backtracking. (c) Navigation towards a goal in an underground parking lot with an incomplete map information.

meters. Since the mapping algorithm takes only the top laser sensor as the input, the parking bumpers are not mapped and a plan can not be constructed to navigate around them. The local reactive navigation uses both sensors as inputs and is capable of detecting the bumpers by using the minimal laser readings from the lower sensor. Therefore, the robot is successful in navigating around these obstacles to arrive at the goal.

From the experiments, we can observe that the navigation system guides the robot towards a local goal obtained in the environment from the laser observations, and, when necessary, the path planner. While not always being able to find the globally optimal path, the navigation system is capable of exploring and navigating in a previously unknown environment and reliably find its way to the global goal. The local navigation is capable of avoiding obstacles in a reactive manner without needing to pre-calculate a path. Combining the local navigation with the planner allows the robot to escape and avoid local optimum as well as facilitate backtracking. The navigation process of the performed experiments in static and dynamic settings is visualized in the accompanying video. The experimentation code as well as higher quality images with videos of the presented and additional experiments are available from a repository at <https://github.com/reiniscimurs/GDAM>.

V. CONCLUSIONS

In this paper, a DRL and planning-based goal-driven fully autonomous mapping navigation system is introduced that

is capable of arriving at a designated goal while recording the environment without direct human supervision. As the experiments show, the system successfully combines reactive local and planned global navigation. Moreover, the task of introducing a neural network-based module for an end-to-end system proves to be beneficial as it allows the robot to move without generating an explicit plan, but its shortcomings are alleviated by the rest of the navigation system. The obtained experimental results show that the proposed system works reasonably close to the optimal solution obtained by the path planner from an already known environment. Additionally GDAM performs with higher reliability by not generating plans from an uncertain map, but rather using direct sensor inputs.

In the current implementation, the local navigation training was performed with the model of the same robot as in the real-life experiments. This allowed for easy transfer of the network parameters to the embedded implementation as the network parameters were optimized for its specifications. In order to generalize to various types of robots, system dynamics could be introduced as a separate input state to the neural network, and training performed accordingly. By only providing robot dynamics, it would be possible to perform local navigation up to its best capabilities. Additionally, a long short term memory architecture could prove beneficial in alleviating the local optimum problem and help avoid obstacles out of the current range of sensors. The design of such a network will be the next step of the ongoing research.

REFERENCES

- [1] Khalid Yousif, Alireza Bab-Hadiashar, and Reza Hoseinnezhad. An overview to visual odometry and visual slam: Applications to mobile robotics. *Intelligent Industrial Systems*, 1(4):289–311, 2015.
- [2] Spyros G Tzafestas. Mobile robot control and navigation: A global overview. *Journal of Intelligent & Robotic Systems*, 91(1):35–58, 2018.
- [3] Masashi Sugiyama. *Statistical reinforcement learning: modern machine learning approaches*. CRC Press, 2015.
- [4] Douglas Aberdeen et al. *Policy-gradient algorithms for partially observable Markov decision processes*. PhD thesis, The Australian National University, 2003.
- [5] Alexander Zelinsky. A mobile robot navigation exploration algorithm. *IEEE Transactions of Robotics and Automation*, 8(6):707–717, 1992.
- [6] Hartmut Surmann, Andreas Nüchter, and Joachim Hertzberg. An autonomous mobile robot with a 3d laser range finder for 3d exploration and digitalization of indoor environments. *Robotics and Autonomous Systems*, 45(3-4):181–198, 2003.
- [7] Tao Chen, Saurabh Gupta, and Abhinav Gupta. Learning exploration policies for navigation. *arXiv preprint arXiv:1903.01959*, 2019.
- [8] Raul Mur-Artal and Juan D Tardós. Orb-slam2: An open-source slam system for monocular, stereo, and rgb-d cameras. *IEEE Transactions on Robotics*, 33(5):1255–1262, 2017.
- [9] Chao Yu, Zuxin Liu, Xin-Jun Liu, Fugui Xie, Yi Yang, Qi Wei, and Qiao Fei. Ds-slam: A semantic visual slam towards dynamic environments. In *2018 IEEE/RSJ International Conference on Intelligent Robots and Systems (IROS)*, pages 1168–1174. IEEE, 2018.
- [10] Linyan Cui and Chaowei Ma. Sof-slam: A semantic visual slam for dynamic environments. *IEEE Access*, 7:166528–166539, 2019.
- [11] Bo Li, Yingqiang Wang, Yu Zhang, Wenjie Zhao, Jianyuan Ruan, and Ping Li. Gp-slam: laser-based slam approach based on regionalized gaussian process map reconstruction. *Autonomous Robots*, pages 1–21, 2020.
- [12] Guolai Jiang, Lei Yin, Guodong Liu, Weina Xi, and Yongsheng Ou. Fft-based scan-matching for slam applications with low-cost laser range finders. *Applied Sciences*, 9(1):41, 2019.
- [13] Kirill Krinkin, Anton Filatov, Art yom Filatov, Artur Huletski, and Dmitriy Kartashov. Evaluation of modern laser based indoor slam algorithms. In *2018 22nd Conference of Open Innovations Association (FRUCT)*, pages 101–106. IEEE, 2018.
- [14] Zhuli Ren, Liguang Wang, and Lin Bi. Robust gicp-based 3d lidar slam for underground mining environment. *Sensors*, 19(13):2915, 2019.
- [15] Marek Pierzchała, Philippe Giguère, and Rasmus Astrup. Mapping forests using an unmanned ground vehicle with 3d lidar and graph-slam. *Computers and Electronics in Agriculture*, 145:217–225, 2018.
- [16] Menggang Li, Hua Zhu, Shaoze You, Lei Wang, and Chaoquan Tang. Efficient laser-based 3d slam for coal mine rescue robots. *IEEE Access*, 7:14124–14138, 2018.
- [17] Xiao Liang, Haoyao Chen, Yanjie Li, and Yunhui Liu. Visual laser-slam in large-scale indoor environments. In *2016 IEEE International Conference on Robotics and Biomimetics (ROBIO)*, pages 19–24. IEEE, 2016.
- [18] Shao-Hung Chan, Ping-Tsang Wu, and Li-Chen Fu. Robust 2d indoor localization through laser slam and visual slam fusion. In *2018 IEEE International Conference on Systems, Man, and Cybernetics (SMC)*, pages 1263–1268. IEEE, 2018.
- [19] Zhe Zhang, Shaoshan Liu, Grace Tsai, Hongbing Hu, Chen-Chi Chu, and Feng Zheng. Pirvs: An advanced visual-inertial slam system with flexible sensor fusion and hardware co-design. In *2018 IEEE International Conference on Robotics and Automation (ICRA)*, pages 1–7. IEEE, 2018.
- [20] Takafumi Taketomi, Hideaki Uchiyama, and Sei Ikeda. Visual slam algorithms: a survey from 2010 to 2016. *IPSI Transactions on Computer Vision and Applications*, 9(1):16, 2017.
- [21] Maksim Filipenko and Ilya Afanasyev. Comparison of various slam systems for mobile robot in an indoor environment. In *2018 International Conference on Intelligent Systems (IS)*, pages 400–407. IEEE, 2018.
- [22] D. W. Ko, Y. N. Kim, J. H. Lee, and I. H. Suh. A scene-based dependable indoor navigation system. In *2016 IEEE/RSJ International Conference on Intelligent Robots and Systems (IROS)*, pages 1530–1537, 2016.
- [23] Lukas von Stumberg, Vladyslav Usenko, Jakob Engel, Jörg Stückler, and Daniel Cremers. From monocular slam to autonomous drone exploration. In *2017 European Conference on Mobile Robots (ECMR)*, pages 1–8. IEEE, 2017.
- [24] Haiming Gao, Xuebo Zhang, Jian Wen, Jing Yuan, and Yongchun Fang. Autonomous indoor exploration via polygon map construction and graph-based slam using directional endpoint features. *IEEE Transactions on Automation Science and Engineering*, 16(4):1531–1542, 2018.
- [25] Narcis Palomeras, Marc Carreras, and Juan Andrade-Cetto. Active slam for autonomous underwater exploration. *Remote Sensing*, 11(23):2827, 2019.
- [26] Matan Keidar and Gal A Kaminka. Efficient frontier detection for robot exploration. *The International Journal of Robotics Research*, 33(2):215–236, 2014.
- [27] Wenchao Gao, Matthew Booker, Albertus Adiwahono, Miaolong Yuan, Jiadong Wang, and Yau Wei Yun. An improved frontier-based approach for autonomous exploration. In *2018 15th International Conference on Control, Automation, Robotics and Vision (ICARCV)*, pages 292–297. IEEE, 2018.
- [28] Yujie Tang, Jun Cai, Meng Chen, Xuejiao Yan, and Yangmin Xie. An autonomous exploration algorithm using environment-robot interacted traversability analysis. In *2019 IEEE/RSJ International Conference on Intelligent Robots and Systems (IROS)*, pages 4885–4890. IEEE, 2019.
- [29] Rakesh Shrestha, Fei-Peng Tian, Wei Feng, Ping Tan, and Richard Vaughan. Learned map prediction for enhanced mobile robot exploration. In *2019 International Conference on Robotics and Automation (ICRA)*, pages 1197–1204. IEEE, 2019.
- [30] Lei Tai and Ming Liu. A robot exploration strategy based on q-learning network. In *2016 IEEE International Conference on Real-time Computing and Robotics (RCAR)*, pages 57–62. IEEE, 2016.
- [31] Linhai Xie, Sen Wang, Andrew Markham, and Niki Trigoni. Towards monocular vision based obstacle avoidance through deep reinforcement learning. *arXiv preprint arXiv:1706.09829*, 2017.
- [32] Lei Tai, Giuseppe Paolo, and Ming Liu. Virtual-to-real deep reinforcement learning: Continuous control of mobile robots for mapless navigation. In *2017 IEEE/RSJ International Conference on Intelligent Robots and Systems (IROS)*, pages 31–36. IEEE, 2017.
- [33] Reinis Cimurs, Jin Han Lee, and Il Hong Suh. Goal-oriented obstacle avoidance with deep reinforcement learning in continuous action space. *Electronics*, 9(3):411, 2020.
- [34] Yu Fan Chen, Michael Everett, Miao Liu, and Jonathan P How. Socially aware motion planning with deep reinforcement learning. In *2017 IEEE/RSJ International Conference on Intelligent Robots and Systems (IROS)*, pages 1343–1350. IEEE, 2017.
- [35] Ashwini Pokle, Roberto Martín-Martín, Patrick Goebel, Vincent Chow, Hans M Ewald, Junwei Yang, Zhenkai Wang, Amir Sadeghian, Dorsa Sadigh, Silvio Savarese, et al. Deep local trajectory replanning and control for robot navigation. In *2019 International Conference on Robotics and Automation (ICRA)*, pages 5815–5822. IEEE, 2019.
- [36] Aleksandra Faust, Kenneth Oslund, Oscar Ramirez, Anthony Francis, Lydia Tapia, Marek Fiser, and James Davidson. Prm-rl: Long-range robotic navigation tasks by combining reinforcement learning and sampling-based planning. In *2018 IEEE International Conference on Robotics and Automation (ICRA)*, pages 5113–5120. IEEE, 2018.
- [37] Timothy P Lillicrap, Jonathan J Hunt, Alexander Pritzel, Nicolas Heess, Tom Erez, Yuval Tassa, David Silver, and Daan Wierstra. Continuous control with deep reinforcement learning. *arXiv preprint arXiv:1509.02971*, 2015.
- [38] Jinyoung Choi, Christopher Dance, Jung-eun Kim, Kyung-sik Park, Jaehun Han, Joonho Seo, and Minsu Kim. Fast adaptation of deep reinforcement learning-based navigation skills to human preference. In *2020 IEEE International Conference on Robotics and Automation (ICRA)*, pages 3363–3370. IEEE, 2020.
- [39] Anis Koubaa, Hachemi Bennaceur, Imen Chaari, Sahar Trigui, Adel Ammar, Mohamed-Foued Sriti, Maram Alajlan, Omar Cheikhrouhou, and Yasir Javed. Integration of global path planners in ros. In *Robot Path Planning and Cooperation*, pages 83–102. Springer, 2018.
- [40] S Macenski. On use of the slam toolbox: A fresh (er) look at mapping and localization for the dynamic world, 2019.
- [41] Daniel Loubach da Silva Lubanco, Markus Pichler-Scheder, and Thomas Schlechter. A novel frontier-based exploration algorithm for mobile robots. In *2020 6th International Conference on Mechatronics and Robotics Engineering (ICMRE)*, pages 1–5. IEEE, 2020.